Molecular signatures of resource competition: clonal interference favors ecological diversification and can lead to incipient speciation

Massimo Amicone[+, *] and Isabel Gordo[+, *]

[+]Instituto Gulbenkian de Ciência (IGC)

[*]corresponding authors: mamicone@igc.gulbenkian.pt, igordo@igc.gulbenkian.pt

Short running title

Clonal interactions drive ecotypes formation.

Author contributions

MA and IG designed the study, all authors wrote the manuscript and provided final approval for publication.

Conflict of interest

The authors declare no conflict of interest.

Acknowledgements

The authors acknowledge C Bank and the members of the Evolutionary Dynamics and Evolutionary Biology labs of the IGC for their assistance throughout the development of this work; PR Campos, T Paixão, S Miller, G Sgarlata and R Ramiro for their comments on the manuscript. This work was supported by Portuguese Science Foundation (FCT) Grant PTDC/BIA-EVL/31528/2017; Deutsche Forschungs-gemeinschaft (DFG) Grant SFB 1310; and a cooperation agreement between University of Cologne and Gulbenkian Institute. MA was supported by FCT Grant PD/BD/138735/2018.

Data archival location will be made public upon acceptance.

Abstract

Microbial ecosystems harbor an astonishing diversity that can persist for long times. To understand how such diversity is structured and maintained, ecological and evolutionary processes need to be integrated at similar timescales. Here, we study a model of resource competition that allows for evolution *via de novo* mutation, and focus on rapidly adapting asexual populations with large mutational inputs, as typical of many bacteria species. We characterize the adaptation and diversification of an initially maladapted population and show how the eco-evolutionary dynamics are shaped by the interaction between simultaneously emerging lineages – clonal interference. We find that in large populations, more intense clonal interference fosters diversification under sympatry, increasing the probability that phenotypically and genetically distinct clusters stably coexist. In smaller populations, the accumulation of deleterious and compensatory mutations can push further the diversification process and kick-start speciation. Our findings have implications beyond microbial populations, providing novel insights about the interplay between ecology and evolution in clonal populations.

Keywords: Eco-evolutionary dynamics, clonal interference, resource competition, competitive exclusion, diversification, speciation.

Introduction

Understanding the mechanisms behind the evolution of biodiversity and the formation of communities remains a difficult challenge. One must integrate ecology and evolution over similar timescales, as taken together, they can give rise to phenomena that could not be explained by either alone (Schoener, 2011). The competitive exclusion principle (first stated by Hardin, 1960) theoretically binds the number of species by the number of limiting resources. This principle generated an apparent contradiction between theoretical expectations and observations, often referred to as the "paradox of the plankton" (Hutchinson, 1961). In fact, ecosystems can be replete of diversity even in limiting environments, both in nature (Hutchinson, 1961; Tilman, 1982; Huston, 1994) and in more controlled laboratory conditions (Maharjan *et al.*, 2006; Gresham *et al.*, 2008; Kinnersley, Holben and Rosenzweig, 2009; Herron and Doebeli, 2013; Good *et al.*, 2017). Different theoretical approaches have been adopted to resolve such controversy. One approach is to assume an existing diversity and identify mechanisms that can maintain it. Following this, several ecological properties were proposed to maintain diversity, including heterogeneity in space (Abrams, 1988) and time (Litchman and Klausmeier, 2001), trade-offs on the species' traits (Posfai, Taillefumier and Wingreen, 2017), or gene regulation (Pacciani-Mori *et al.*, 2020). Here we explore a classical model of competition for resources, where extensive diversity can be maintained by a metabolic trade-off (Posfai, Taillefumier and Wingreen, 2017), and ask a different question: in an initially monomorphic population, what diversity can be generated and maintained if the species' traits continuously evolve?

In eco-evolutionary frameworks, mutations generate new genetic variants whose fate depends on the state of the ecosystem and, in turn, their increase in frequency can alter the populations. A common outcome of such eco-evolutionary feedbacks is that evolution limits diversity by reducing the effectiveness of coexistence mechanisms (Edwards *et al.*, 2018). The diversity that would be possible by ecological principles alone, is reduced by selection of the fittest and competitive exclusion. Several studies have produced novel understanding on the evolution of diversity (Dieckmann and Doebeli, 1999; Shoresh, Hegreness and Kishony, 2008; Doebeli, 2011; Kremer and Klausmeier, 2017), but the majority rely on the strong-selection-weak-mutation assumption, i.e. on a timescale separation between ecological and evolutionary

processes (but see Farahpour *et al.*, 2018). The emergence of mutations is assumed to be much slower than the ecological dynamics, thus, before a new lineage arises, the population has already reached ecological equilibrium. While allowing for analytical tractability the weak mutation assumption comes at a cost: it neglects the overlap between multiple evolving lineages – clonal interference. Clonal interference has been extensively observed in microbial communities *in vitro* and *in vivo* (Desai, Fisher and Murray, 2007; Barroso-Batista *et al.*, 2014) and can occur under different regimes of intensity: a weak regime where a few lineages compete for fixation (Philip J. Gerrish & Richard E. Lenski, 1998; Billiard and Smadi, 2020) or one where many different haplotypes segregate (Good *et al.*, 2012). Population genetics models incorporating clonal interference have generated predictions for the adaptation rate, fixation probabilities and genetic diversity in a population (Gerrish and Lenski, 1998; Park and Krug, 2007; Good *et al.*, 2012; de Sousa *et al.*, 2016), yet they typically ignore ecological interactions (but see Good, Martis and Hallatschek, 2018).

When the population size (N) and/or the mutation rate to new beneficial mutations (U_b) are not small (NU_b >>1), multiple lineages can increase in frequency simultaneously, ecologically interact with each other and evolve in non-trivial ways. Although these processes are inevitably intertwined in real ecosystems (Lawrence *et al.*, 2012; Barroso-Batista *et al.*, 2014, 2020; Garud *et al.*, 2019), theoretical work is still needed to investigate how they act in chorus.

Good and colleagues (Good, Martis and Hallatschek, 2018) have recently developed a theoretical work that incorporates ecological and evolutionary mechanisms *via* a combination of frequency-dependent and directional selection. Their eco-evolutionary model is able to reproduce empirical patterns of co-existence and fixation of new mutations in experimentally evolved clonal populations (Good *et al.*, 2017). It also shows how diversification depends on the ratio between the rates of strategy mutations and unconditionally beneficial mutations. However, in order to derive analytical expression for the eco-evolutionary dynamics, the authors have focused on the weak mutation limit NU_b <<1 and only briefly investigated clonal interference.

Here, we study a similar model to that of (Posfai, Taillefumier and Wingreen, 2017; Good, Martis and Hallatschek, 2018) but assume a trade-off that only affects well adapted genotypes (fitness-dependent trade-off) and conduct a more systematic

simulation study of the different mutation regimes, including extensive clonal interference, in large and small populations. We follow an initially isogenic population throughout time and characterize the patterns of adaptation at both phenotypic and genetic levels, by common statistics used to analyze molecular evolution data. We focused only on mutations that affect the ability of consuming resources (instead of differentiating between strategy and unconditionally beneficial mutations) and we do not impose restrictive assumptions on mutation rates and on timescales, as common in other models (Geritz *et al.*, 1998; Shoresh, Hegreness and Kishony, 2008; Good, Martis and Hallatschek, 2018). Albeit at the cost of analytical tractability, our approach is to focus on the phenomena that emerge from the stochastic simulations where many more lineages compete, compared to previous studies (Billiard and Smadi, 2020).

We find that: high levels of intra-specific variation can be generated and maintained via a balance between selection and mutation; functionally distinct clusters of genotypes – ecotypes - can emerge and stably coexist; and the interaction between large mutational inputs and the energetic trade-off can lead to incipient speciation. Taken together, our results describe how clonal populations can give rise to extensive diversity and establish a first form of community, even in simple and constant environments.

Model and Methods

Eco-Evolutionary model

We model the dynamics of a single clonal lineage evolving to consume a set of different substitutable resources, constantly replenished in a well-mixed environment (Fig.1A). Individuals mutate at a rate U (per-genome, per-generation rate of non-lethal mutations) and the fate of the emerging mutations depends on their phenotypic effects, on the resource concentration, on the other individuals present in the environment and on drift.

The underlying dynamics are based on the MacArthur's consumer resource model (Mac Arthur, 1969), recently formalized to explain high levels of diversity in the presence of a metabolic trade-off (Posfai, Taillefumier and Wingreen, 2017) and further extended to study adaptation (Good, Martis and Hallatschek, 2018). Briefly, let M be the number of

types present at time t with densities (*#cells/V*) n_i, *(i=1...M)* and R the number of substitutable resources with input concentrations r_j, *(j=1...R)*. The expected density dynamics of each type are:

$$\frac{dn_i}{dt} = n_i(t)\left(\sum_{j=1}^{R} \frac{\alpha_j^{(i)} r_j}{\sum_{k=1}^{M(t)} n_k(t)\cdot\alpha_j^{(k)}} - \delta\right) \quad (1)$$

where $\alpha_j^{(i)}$ represents the consumption rate of resource j by type i and δ is the death rate. The resource amounts are constant in this model since, as *Posfai et al.*, we assume that metabolic reactions occur much faster than cell division (Posfai, Taillefumier and Wingreen, 2017).

We assume a finite amount of energy available for each cell and limit their ability of consuming resources by an energetic constraint (E):

$$0 \leq \sum_{j=1}^{R} \alpha_j^{(i)} \leq E\ ,\ \forall i = 1, \dots, M \quad (2)$$

Under this assumption, E acts as an upper bound and not as a fixed energy budget, as previously investigated (Posfai, Taillefumier and Wingreen, 2017; de Oliveira, Amado and Campos, 2018; Amado and Campos, 2019). Assuming equally supplied resources ($r_j = r\ \forall j$) and unitary energy, volume and death rate (*E, V, δ=1*), the population size is *N=Rr*.

We model an initial isogenic population ($M(t_0)$ =1) with given traits $\vec{\alpha}^{(1)}$ and allow for mutations that change the heritable traits and give rise to new genotypes. Every generation, each genotype *i (i=1...M(t))* will generate a Poisson-distributed number of mutants with expected value $n_i(t) \cdot U$. Assuming an infinite site model, a mutation on genotype *i* will result into a new individual with unique genotype (i') whose phenotypes differ from the parental traits by a small amount: $\vec{\alpha}^{(i')} = \vec{\alpha}^{(i)} + \vec{\Delta},\ \vec{\Delta} \in \mathbb{R}^R$.

The mutation effects are drawn from a normal distribution as follows:

$$\vec{\Delta}: \begin{cases} \Delta_j \sim N(0,\sigma), \text{trait } j \text{ sampled from } \{1, \dots, R\} \\ \Delta_z \sim N(0, \rho\cdot\sigma), \text{for all traits } z \neq j \end{cases}$$

If ρ *=1*, a mutation changes all the traits with equal probability. If 0< ρ *<1*, mutations target one trait (randomly sampled with probability *1/R*), but partially alter the other ones. If ρ *=0*, a mutation only changes a single trait. The parameter ρ modulates

different degrees of trait interdependence or equivalently the pleiotropic effect of mutations, while the parameter σ modulates the magnitude of the mutation effects (see Fig. 1B).

In order to respect the boundary condition (2), we assumed that: i) mutations leading to negative values of α_j are loss of function and thus assigned α_j=0; ii) mutations that do not respect the energy constraint cannot exist, therefore Δ_j are drawn until the upper limit of (2) is satisfied.

In the limit of discrete time steps, we define the selection acting on genotype i at time t, $s_i(t)$, as the expected increase in abundance in the absence of drift, such that $E[n_i(t+1)] = n_i(t)\big(1 + s_i(t)\big)$, and from (1):

$$s_i(t) = \sum_{j=1}^{R} \frac{\alpha_j^{(i)} r_j}{\sum_{k=1}^{M(t)} n_k(t) \cdot \alpha_j^{(k)}} - \delta \,. \tag{3}$$

The fate of each genotype depends on its ability to consume each of the resources and on the ecosystem's ecology.

To simulate drift, we draw the final abundances via multinomial sampling with probabilities $\frac{E[n_i(t+1)]}{n_{tot}}$ $\forall i=1...M(t)$. Every generation, the number of genotypes $M(t+1)$ is updated together with the relative abundances, traits and phylogeny.

Numerical simulations

In each simulation, an initially maladapted ($\sum_{j=1}^{R} \alpha_j^{(1)} = 0.1$) and monomorphic population undergoes the eco-evolutionary process described above for 10^4 generations, enough to reach phenotypic equilibrium. We focus on the role of different mutation types and regimes (Fig. 1B-C), thus, the main results are obtained via exploring different ranges of the parameters N, U, σ and ρ, whose values are specified along the text. Each combination of parameters was simulated in 100 independent replicates to obtain the statistics of diversity. In order to disentangle the role of the energetic constraint assumption, we also simulated adaptation under selection but without any boundary condition (or equivalently E=+∞ for (2)). The algorithm was written in *R* (*version 3.6.1*) and the results analyzed in *RStudio*. We validated the code by comparing simulations outcomes against well-known theoretical expectations from

population genetics (see Fig. S1). The code for the simulations is available at https://figshare.com/s/a85bfd4b9f64afaeba1b.

Neutral mutation model

Neutral theories provide null expectations for the genetic diversity within a population, assuming that this population has reached equilibrium. As the time to reach such equilibrium is proportional to the population size (N), neutral predictions are not adequate for "short-term" adaptation of large populations ($T \ll N$), e.g. experimental evolution with bacterial populations. Thus, we run simulations with only drift, for the same time as the selection case ($T = 10^4$). These out-of-equilibrium simulations help disentangling the contribution of neutral processes to the patterns that we observe during adaptation under selection.

Under the neutral mutation model, genotypes acquire mutations with the same trait effects and probability as described before, but their growth probabilities are equal and do not depend on the phenotypes. Modelling the explicit α_j under neutrality, instead of assuming that the mutations have no effect ($\Delta_j=0$), allows for both genetic and phenotypic comparisons with the model of selection.

Phenotypic and genotypic diversity

Within a population, each type i is characterized by a vector of its consumption traits $(\alpha_1^{(i)}, \ldots, \alpha_R^{(i)})$ and a vector of the mutations that gave rise to it, each with a unique identifier (e.g. the vector [1,2,7,10] represents genotype 10 whose ancestors are, in order, genotypes 7,2 and 1, and 1 is the ancestor common to every type). From this implementation we can reconstruct the entire phylogeny of a population at any time point and map it on the phenotypic space.

We measure the genetic diversity of a population by the average pairwise genetic distance π_G in a sample of m individuals: $\pi_G(m) = \frac{\sum_{(i,j)} d_G(i,j)}{\binom{m}{2}}$, where $m=100$ and $d_G(i,j)$ is the number of mutations that separate genotype i from j. From π_G and the number of segregating sites in the sample, we further compute another population genetics statistic: Tajima's D (Tajima, 1989). The expected value of D at equilibrium is: zero, without selection; positive, under divergent selection; and negative, under purifying selection. However, as the time of our focus (10^4 generations) is much shorter than that required to achieve equilibrium ($\sim N=10^7$), only relative comparisons are meaningful.

At the functional level, we compute the average pairwise phenotypic distance π_P, defined as: $\pi_P(m) = \frac{\sum_{(i,j)} d_E(i,j)}{\binom{m}{2}} \cdot \frac{1}{\sigma}$, where d_E is the classical Euclidean distance and it is normalized σ, for a direct comparison with π_G. For each of the evolved populations, we identified functional clusters from their phenotypic distribution, via the mean shift clustering algorithm (Cheng, 1995), implemented through the *R* package *meanShiftR* version 0.53 (Lisic, 2018) (see Appendix S2 in Supporting Information).

Results

Competition-driven diminishing return and the rate of adaptation

The initially monomorphic population, which is poorly adapted, is expected to acquire mutations that improve the ability to consume the available resources and to advance in the phenotypic space towards better adapted states. Our first aim is to identify what influences the speed of this adaptive process.

Under the competition for resources set by (1), how does selection change over time and with the genetic composition of the population? Selection acting on an emerging genotype i is given by (3) and depends on the population investment on each resource j: $e_j^{(M(t))} := \sum_{i=1}^{M(t)} n_i(t) \cdot \alpha_j^{(i)}$. Let us first simplify the problem by considering a monomorphic ($M=1$) population whose phenotypes ($\vec{\alpha}$) mirror the resource input proportions: $\frac{\alpha_j}{\sum_k^R \alpha_k} = \frac{r_j}{\sum_k^R r_k}, \forall j = 1, \dots, R$ which consists of the local optimal strategy for a given energetic investment ($\sum_k^R \alpha_k$). In the absence of mutations, such population at equilibrium satisfies:

$$e_j^{(1)} = r_j \cdot \sum_{k=1}^R \alpha_k \qquad \forall j = 1, \dots, R. \tag{4}$$

Now consider a mutant that emerges from this population with phenotypes $\vec{\alpha}_{mut} = \vec{\alpha} + \vec{\Delta}$. From (3) and (4) it follows that the selection acting on such mutant is:

$$s_{mut}(\vec{\alpha}, \vec{\Delta}) = \frac{\sum_j^R \Delta_j}{\sum_j^R \alpha_j}. \tag{5}$$

While bigger steps result in stronger selection, equation (5) also implies that the same mutations are subject to weaker selection when emerging on a better adapted

background. Thus, competition-driven selection in our system, as in (Good, Martis and Hallatschek, 2018), exhibits diminishing return epistasis - the benefit decline in populations with higher mean fitness – consistent with many empirical observations in microbial populations (Chou *et al.*, 2011; Kryazhimskiy *et al.*, 2014; Schoustra *et al.*, 2016; Wünsche *et al.*, 2017).

Because we assume phenotypic changes follow a normal distribution, their additive effect will also follow a normal distribution: $\sum_j^R \Delta_j \sim N(0, \sigma^*)$ where $\sigma^* = \sigma\sqrt{(R-1)\cdot\rho^2+1}$; this implies that stronger pleiotropic effects lead to stronger selection. From the continuous univariate distribution theory (Johnson *et al.*, 1994) we can retrieve the expected beneficial mutation effect ($E[\sum_j^R \Delta_j]$) and, from (5), compute the corresponding expected selection coefficients ($E[s^+]$) for varying values of $\sum_j^R \alpha_j$ (see Appendix S1 in Supporting Information). Figure 2A shows how the strength of positive selection decreases for better adapted genetic backgrounds across different σ and ρ conditions. It is important to note that the diminishing return epistasis in this model is not due to the energy constraint; nonetheless, such boundary condition makes the deleterious mutations more common (see Fig. S2 and Appendix S1) and further slows down the rate of adaptation of these well adapted populations (inset in Fig. 2A).

Next, we tested how well the approximation obtained by assuming monomorphic populations at consecutive equilibria, predicts what happens in regimes where the adapting populations are polymorphic and out of equilibrium. From the simulations with *NU=100* and two resources, we computed the average population trait sum $\hat{\alpha}(t) := \frac{\sum_i^{M(t)}\left(\alpha_1^{(i)}+\alpha_2^{(i)}\right)\cdot n_i(t)}{N}$ and the expected beneficial selection coefficient as $E[s^+|\hat{\alpha}] = \frac{E[\Delta_1+\Delta_2|\hat{\alpha}]}{\hat{\alpha}}$. We then compare this expectation with the mean beneficial selection observed in the simulations, during the first 300 generations. The strength of selection acting on polymorphic populations follows the predicted diminishing return pattern, but is often underestimated (Fig. 2B). In fact, it decreases with the mean population phenotype $\hat{\alpha}$, but it increases with the population phenotype variance (Fig. S3).

Numerical simulations further allow us to link the mutation types with the speed of phenotypic adaptation: larger phenotypic changes imply stronger selection, resulting in

279 faster adaptation (Fig. 2C). We find that, when time is scaled by $\int_{\hat{\alpha}(t0)}^{1} E[s^{+}|\hat{\alpha}]d\hat{\alpha} \cdot \sigma^{*}$,
280 the populations' mean phenotype moves with similar velocity, demonstrating that both
281 the complex form of selection and the mutation type mediate the speed of adaptation
282 (Fig. 2D and Appendix S1).

283 Finally, the simulations show that, as expected, larger mutational inputs accelerate
284 phenotypic adaptation and more rapidly lead the populations to a quasi-neutral regime
285 where beneficial mutations are rare and of small effects ($P(s^{+}) \cdot E[s^{+}] \sim \frac{1}{N}$) (Fig. 2E).

286 Taken together, these results describe the interactions between the distribution of
287 mutation effects, the competition-dependent selection and the energetic constraint and
288 will help understand the emerging genetic and phenotypic diversity (see below).

289 **Number of coexisting genotypes**

290 During the adaptation of an initially monomorphic population, *de novo* mutations
291 generate polymorphism but at the same time purifying selection tends to reduce such
292 diversity. How many genotypes are generated and maintained under competition for
293 resources? Under the parameters explored in the simulations we observe that: after an
294 initial burst of diversity, the mean number of genotypes first declines and later plateaus
295 around a value below that obtained under neutrality (Fig. 3A). The drop in the mean
296 number of genotypes is due to the energetic constraint, as populations evolving under
297 neutrality or without such boundary do not suffer any decline (Fig. S4). When the
298 populations' phenotypes approach the energetic constraint, beneficial mutations
299 become rarer and selection reduces the number of coexisting genotypes (Fig. S4).
300 Despite the more abundant deleterious mutations, the populations can maintain a
301 dynamic balance between the mutations that are purged by purifying selection and the
302 newly emerging ones (inset of Fig. 3A).
303 When we summarize the populations' composition (at generation 10000) by calculating
304 the average rank abundance distributions of the genotypes (instead of the species,
305 Whittaker, 1965) we observe that few genotypes dominate the population (frequency
306 above 1%) and the rest persists at low abundance (Fig. 3B). As the mutational input
307 increases, the effect of selection becomes more pronounced as seen by stronger
308 deviations from the rank abundance distribution observed under neutrality. As
309 expected, under purifying selection less genotypes can be maintained at intermediate

abundances (Haldane and Fisher, 1931; Wright, 1938). Under the conditions simulated here, populations maintain a dynamically stable genotype richness which increases linearly with the mutational input NU, and it's about 1/3 of that expected under neutrality (with σ=0.05) (Fig.3C). Thus, clonal populations with large NU and strong selection ($N\sigma$ >>1) can maintain high levels of intraspecific variation under adaptation to few resources. However, we were unable to find an approximation to predict the number of genotypes, M^*, across different combinations of N, U and σ, indeed M^*, deviates from NU/σ - the expected mean number of deleterious mutations under mutation-selection balance in a simple model of constant negative selection (Haigh, 1978).

Population diversification into ecotypes

In this model, adapting populations consist of a cloud of many genotypes and we now characterize the phenotypic structures of these clouds. If a population consisted of a single genotype, the optimal strategy (hereafter Ω) would be to have the trait values that mirror the resource supply proportions $\left(\alpha_j = \frac{r_j}{r_{tot}}, \forall j = 1, \dots, R\right)$, as represented by the star in Figs. 1-4. Such state cannot be invaded by any mutant ($s_{mut}^{\Omega} \leq 0$), thus excluding diversity. However, if polymorphism already exists and metabolic trade-off is assumed, a large collection of types can stably coexist if they are distributed around Ω (Posfai, Taillefumier and Wingreen, 2017). Thus, we now ask the simple question: if there is no initial polymorphism and mutation is the only source of variation, will an initially maladapted population evolve a single strategy or multiple ones?

The simulations show alternative stable states: due to the stochastic nature of mutation, populations can evolve to either one or to multiple strategies, even if adapting under exactly the same conditions (e.g. Fig. 4A). Remarkably, the same ancestral genotype can give rise to many functionally similar genotypes (Fig. 4A, left panel), or can diversify into different ecotypes (Cohan, 2002): clusters of genotypes with distinct metabolic preferences, capable of coexisting indefinitely (Fig. 4A, right panel).

We now investigate the conditions favoring such ecotype diversification, across several mutational inputs and in the regime of strong selection ($N\sigma$ 1). Using the mean shift clustering algorithm (Cheng, 1995) to group each adapted population into functional clusters (see details in *Methods* and Appendix S2), we find that the proportion of

342 populations that evolved into 1, 2 or more statistically distinct clusters, depends on the
343 underlying mutation parameters. Under regimes of larger mutational input (i.e. more
344 intense clonal interference) ecotypes with distinct preferences more likely emerge and
345 coexist (Fig. 4B). Importantly, when NU is very large, the system can support
346 supersaturation: the number of ecotypes inferred by the mean shift algorithm can
347 exceed the number of limiting resources (Fig. 4B). This result is confirmed when using
348 the k-means clustering algorithm (MacQueen, 1967) (data not shown). Although
349 difficult to achieve, supersaturation is stable if the clusters' fitness differs by a relatively
350 small amount ε (with $\varepsilon < \frac{\log(N)}{N}$) (Posfai, Taillefumier and Wingreen, 2017), but until
351 then, the fate of supersaturated populations will be subjected to selection and *de novo*
352 mutation (inset of Fig.4B for an example of the fate of a specific population).
353 The probability of diversification (P) – computed as the proportion of populations that
354 evolved more than one cluster – is close to zero when $NU<1$ but significantly increases
355 when $NU \geq 1$. We summarize the increase observed in these simulations by the logistic
356 function: $P = \frac{1}{1+e^{a(\ln(NU)-b)}}$ (see Fig. 4C and Tables S1-2). Note that the formation of
357 ecotypes is not due to neutral processes as the populations adapting under neutrality
358 did not diversify during the first 10000 generations simulated (Fig. 4C).
359 Not only the rate influences the diversification process (Fig. 4B) but also the type of
360 mutations (Fig. 4C): under intense clonal interference, larger mutation effects (σ)
361 and/or smaller pleiotropic effects (ρ) promote the formation of multiple ecotypes (Fig.
362 4C, Fig S5 and S6).
363 In summary, during the process of adaptation studied in these simulations, different
364 qualitative outcomes can be observed: i) when the input of new mutations is low, the
365 fittest genotype recurrently takes over as a cloud of genotypes until the population
366 reaches a distribution around the generalist strategy that mirrors the resource supply
367 (e.g. Video S1); ii) but when NU is large enough, the initial availability of many beneficial
368 mutations causes adaptive radiation, opens the door for several genotypes to coevolve
369 and for distinct ecotypes to stably coexist (e.g. Video S2).
370

371 **The genetic signature of diversification**

372 We characterized the adapting populations by calculating their average pairwise genetic
373 (π_G) and phenotypic (π_P) distances within populations. Both π_G and π_P increase with NU

374 and always exceed the neutral simulations (Fig. 5A). However, genetic diversity does
375 not necessarily imply functional diversity as some populations are observed to
376 converge to similar phenotypes (see examples in Fig. S7) after an initial increase in
377 diversity. Larger pleiotropy (ρ) in mutation effects reduces phenotypic diversity (Fig.
378 5A) and can foster a higher fraction of populations to exhibit phenotypic convergence.
379 In the populations evolved with large *NU*, π_P and π_G correlate ($\pi_P \sim 0.7\,\pi_G$, Fig. S8 top
380 panel), but strong pleiotropy reduces the correlation (Fig. S8 bottom panel), explaining
381 why fewer clusters are generated under this condition (Fig. 4C).
382 Can we infer ecotype formation from the genetic composition of a population? The
383 Tajima's D statistic, that compares the pairwise genetic diversity with the number of
384 segregating mutations in a sample, is meant to distinguish between different forms of
385 selection. D is expected to be negative under recurrent sweeps or weak purifying
386 selection, and positive under balancing selection (Tajima, 1989). We thus expect that
387 the populations where stable ecotypes have formed show positive D values. Overall, the
388 populations that diversified into multiple phenotypic clusters have on average larger π_P,
389 π_G, Tajima's D and fewer fixations (Fig. 5B, Mann-Whitney p-values < 10^{-9} for each of
390 them). However, the distributions of Tajima's D greatly overlap and require extra care
391 in the study of out of equilibrium populations. In our simulations, under the
392 accumulation of neutral mutations, larger mutational inputs push D towards negative
393 values by generating larger numbers of segregating sites (Fig. S10). But, under selection,
394 this can be counteracted by the increase of π_G, and D presents a wider distribution and a
395 non-monotonic relation with *NU* (Fig. S10). This makes the interpretation of the
396 Tajima's D more complex, and may help explain the overlap between the distributions
397 of D in the simulation results of Fig. 5B.
398 The genetic diversity alone is better at discriminating the populations with multiple or
399 single ecotypes (Fig. 5B), but its predictive power becomes less accurate in the regimes
400 with larger pleiotropic effects (Fig. S9), due to the increased phenotypic convergence
401 discussed above. Nevertheless, while with cross-sectional data it is difficult to establish
402 that ecotypes have formed, with time series data the signal can be clearer (e.g. Fig. S7
403 where π_G is large and D is positive along time). Statistics on population genomic data,
404 together with functional measurements, should allow to identify populations that
405 undergo ecological diversification.
406

407 **Small population size and accumulation of deleterious mutations can lead to**
408 **speciation**

409 So far, we have investigated adaptation in large populations with strong selection,
410 where deleterious mutations hardly ever fix as most stay at low frequencies. Now, we
411 explore simulations with different population sizes but under the same range of
412 mutational inputs as before (NU=0.1-500). When $N = 10^5, 10^7$ or 10^9 the probability of
413 diversification increases consistently (Table S3), confirming its relation with the
414 parameter NU in regimes with large populations (Fig.6A). Differently, when $N = 10^3$ the
415 probability of diversification shows a sharper increase (Fig. 6A, Table S3) as all the
416 populations present multiple phenotypic clusters when $NU \geq 100$. This is due to a
417 different diversification process which requires the accumulation of deleterious
418 mutations as we will explain. When $N = 10^3$ and $NU \geq 100$, we expect that deleterious
419 mutations of a given effect s can accumulate under the action of Muller's ratchet
420 (Felsenstein, 1974). In fact, in such regime, assuming constant $s = \sigma$ (here $\sigma = 0.05$), it
421 follows that $sNe^{-\frac{U}{s}} < 10$, and the Muller's ratchet should click in the time scale of our
422 simulations (Gordo and Charlesworth, 2000). Contrarily, when $N = 10^5, 10^7$ or 10^9, it
423 follows that $sNe^{-\frac{U}{s}} \gg 10$, and the deleterious mutations should fix only in
424 infinitesimally large time (Fig. S11). Furthermore, (Etheridge, Pfaffelhuber and
425 Wakolbinger, 2012) showed that the ratchet can click when the parameter $\gamma :=$
426 $\frac{NU}{Ns \cdot \ln(NU)} > 0.5$, in a constant s model. If we fix $s = \sigma$ and $N = 10^3$, this threshold
427 condition occurs when $\ln(NU) > 4.8$ (dotted line in Fig. 6A), consistent with the abrupt
428 change in the observed probability of diversification and suggesting that when the
429 ratchet turns, deleterious mutations will allow phenotypic clusters to form.
430 Studying large and small populations with different mutation rates (U=10^{-5} or U=10^{-1},
431 respectively) but equal mutational input (NU=100), we compare the two qualitatively
432 different regimes. Fig. 6B shows how the ratchet reduces the average trait sum of the
433 small populations relative to the large populations (case where the ratchet does not
434 turn). Because in this parameter range beneficial mutations are still common (Fig 6B,
435 right panel), their effect balances that of the deleterious mutations and the mean fitness
436 equilibrates at intermediate levels (as in Goyal *et al.*, 2012). While the mean fitness is
437 constant, the phenotypic distribution becomes bimodal. Contrarily to what was
438 previously observed in the large populations (diversification in the early steps of

adaptation and then long-term stabilization), in these smaller populations ($N = 10^3$) with large mutation rate ($U = 10^{-1}$), diversification happens after the energetic boundary in reached (Fig. 6C). The continuous accumulation of deleterious and compensatory mutations drives the clusters apart until they reach the specialist extremes and finally stabilize (see an example in Fig. 6C and Fig. S12). Thus, in the small populations with large mutational inputs, ecological diversification can maximize the functional diversity within the population, lead to a continuous increase of genetic diversity and push the Tajima's D values well above neutral expectations (Fig. 6D). This process should in principle lead to incipient speciation in the long run.

Discussion

Microbial communities are vital for humans and many other host species (Nicholson *et al.*, 2012; Sunagawa *et al.*, 2015). Emerging observations of evolution in such ecosystems (Barroso-Batista *et al.*, 2014; Garud *et al.*, 2019; Zhao *et al.*, 2019) motivate new theories where the mechanisms that generate diversity involve complex forms of selection and clonal interference (Gordo, 2019). We propose that a simple eco-evolutionary model of resource competition, describing the mechanisms behind ecological divergence, can help understand diversity within ecosystems. This framework can be generalized to incorporate other evolutionary mechanisms, such as other forms of selection (Good, Martis and Hallatschek, 2018), transmission and horizontal gene transfer, and can serve to bridge an existing gap between ecology and population genetics.

Population genetics models of clonal interference have greatly advanced our understanding of microbial adaptation (Gerrish and Lenski, 1998; Park and Krug, 2007; Good *et al.*, 2012; de Sousa *et al.*, 2016). However, clonal interference is rarely considered in theoretical studies of ecosystems (Farahpour *et al.*, 2018), even though it greatly impacts the evolution of microbes within real communities (Barroso-Batista *et al.*, 2014) and may be relevant in key ecosystems such as the human microbiota (Zhao *et al.*, 2019). Commensal species in the gut have large population sizes $\sim 10^8$ cells/g. If each bacterium mutates in the gut as it does in the laboratory (Drake, 1991), then each gram of material will host around 10^5 new mutant cells every generation. Even if only

470 0.1% brings up a benefit (Perfeito *et al.*, 2007), clonal interference still extensively
471 affects the gut microbiota dynamics.

472 Here we have studied an ecological model where clones do not compete for fixation but
473 for resources. Modeling competition explicitly allows to make testable predictions
474 about different measures of diversity as both the traits and genomes can now easily be
475 studied. We show that clonal interactions can drive an initial monomorphic population
476 to polymorphism with distinct ecotypes, deviating from the simple expectation of
477 adapting to a single optimal phenotype (Fig. 4 and Fig.6).

478 Taking the MacArthur model, it was previously demonstrated that metabolic trade-offs
479 promote coexistence of more species than resource types, thus overcoming the
480 competitive exclusion principle (Posfai, Taillefumier and Wingreen, 2017). Extensions
481 of this framework already demonstrated its power in recapitulating experimental
482 results from studies of soil, plant (Goldford *et al.*, 2018) or even mammalian gut
483 microbiotas (Leónidas Cardoso *et al.*, 2020). And further extensions provided new
484 analytical results of how populations can adapt under competition for resources and
485 demonstrated that directional selection can limit ecological diversification (Good,
486 Martis and Hallatschek, 2018). This pattern is also observed in our simulations as we
487 find that stronger pleiotropy, which causes stronger directional selection, limits the
488 emergence of clusters (Fig. 4C). Our work differs from the latter by focusing on
489 mutations that alter the metabolic strategies and by quantifying the phenomena that
490 emerge out of equilibrium. We show that under clonal interference, the outcome of
491 phenotypic adaptation is probabilistic, whereby the populations can evolve paths that
492 were not observed under equilibrium assumptions. We further observe that small
493 populations with large mutation rates will diversify by the accumulation of deleterious
494 mutations and generate different species-like lineages.

495 Trade-offs are commonly assumed and expected to affect evolutionary trajectories
496 (Farahpour *et al.*, 2018; Amado and Campos, 2019), but this is not always observed.
497 While many empirical results have confirmed the role of trade-offs during adaptation
498 (Bell and Reboud, 1997; Bull, Badgett and Wichman, 2000; Turner and Elena, 2000;
499 Dykhuizen and Dean, 2004; Greene *et al.*, 2005; Duffy, Turner and Burch, 2006; Coffey *et*
500 *al.*, 2008; Ward, Perron and MacLean, 2009; Bailey and Kassen, 2012; Li, Petrov and

501 Sherlock, 2019), others did not find evidence for any (Reboud and Bell, 1997; Kassen
502 and Bell, 1998; Turner and Elena, 2000; Trindade *et al.*, 2009; Bedhomme, Lafforgue
503 and Elena, 2012). Here we assumed a linear trade-off in the form of an energetic
504 constraint, which only affects well adapted genotypes. Thus, in our model the
505 observation of a trade-off depends on the time at which it is measured. It would be
506 interesting to test for trade-offs at different times during adaptation, as this could
507 explain some of the contrasting findings outlined above. Compatible with this
508 hypothesis, a trade-off in *Escherichia coli* ability to grow in the presence of both glucose
509 and lactose was found, but it only emerged after a period of constraint-free adaptation
510 (Satterwhite and Cooper, 2015). We find that in large populations, the metabolic trade-
511 off in the resource consumption is not required for the formation of distinct ecotypes
512 but it promotes their stable coexistence (Fig. 4, S7 and Video S2).

513 In many ecosystems, the coexisting types seem to outnumber the limiting resources,
514 and, solving this contention has motivated numerous studies. Previous eco-evolutionary
515 analysis suggest that adding evolutionary changes confirms (Edwards *et al.*, 2018) or
516 even exacerbates (Shoresh, Hegreness and Kishony, 2008) this paradox. Perhaps
517 surprisingly, our simulations show that large mutational inputs maintain a dynamically
518 stable number of types that overcome the competitive exclusion (Fig. 3). And at the
519 functional level, diversity generally respects the exclusion principle (number of types ≤
520 number of resources) but with exceptions: in a regime of strong clonal interference, the
521 number of extant ecotypes can be larger than the number of limiting resources (Fig. 4B).

522 We show that the process leading to ecological diversification is strongly influenced by
523 the underlying molecular parameters: regimes of low clonal interference (NU <1) lead
524 to the evolution of a single generalist population, but large mutational inputs ($NU \geq 1$)
525 more likely lead to the formation of two or more differentially specialized ecotypes (Fig.
526 4 and Video S1-S2). Our analysis demonstrates that large mutation effects and weak
527 pleiotropy foster ecological diversification (Fig. 4C). Different pleiotropic effects are
528 meant to represent different interactions between the traits under selection. If the
529 available resources are similar (e.g. chemical composition) and/or the metabolic
530 processes involved in their consumption share many genes, this could increase the
531 chances that a mutation affects the two traits simultaneously leading to large
532 pleiotropy. Contrarily, less related resources could involve more independent effects

533 leading to smaller pleiotropy, promoting diversification (Fig. 4C). This interpretation
534 could explain why adaptive diversification occurred in some experimental evolution
535 setups (Friesen *et al.*, 2004; Sandberg *et al.* 2017) but was not observed in others
536 (Satterwhite and Cooper, 2015; Sandberg *et al.* 2017). In agreement with this
537 hypothesis, Sandberg and colleagues showed that evolving on less metabolically related
538 resources promoted ecological diversification (Sandberg *et al.* 2017).

539 Sympatric diversification can be observed experimentally and predicted by theoretical
540 models (Friesen *et al.*, 2004). The framework of adaptive dynamics has been extensively
541 used in this context as it describes evolution on fitness landscapes that change
542 dynamically due to frequency-dependent interactions (Geritz *et al.*, 1998; Doebeli,
543 2011). However, these models lack the explicit mechanism of competition for resources
544 and are based on equilibrium assumptions: the populations first evolve to an
545 equilibrium state before diversification occurs, as explained by the concept of
546 evolutionary branching points. Our individual-based model, in contrast, allows to follow
547 adaptation of populations that undergo strong non-equilibrium dynamics and can
548 accumulate deleterious mutations if they are small (Fig.6). Previous studies (Rosindell,
549 Harmon and Etienne, 2015; Ispolatov, Madhok and Doebeli, 2016) highlighted how
550 considering evolution at the individual level is necessary to fully understand the
551 adaptation process.

552 We find that the genetic diversity of a population can be used to predict the underlying
553 phenotypic structure, but with limitations (Fig. 5). Other statistics based on genetic data
554 (such as the Tajima's D) can help in understanding the diversity structure, especially if
555 these are assayed along time (Fig.6).

556 The model studied here serves as a first step at integrating phenotypic and genetic data
557 in a relatively simple environment. It predicts that the typical high mutational input of
558 bacterial species and cancer cells, coupled with an energetic constraint, is a mechanism
559 capable of generating functionally diverse clonal communities. Future frameworks
560 addressing microbial ecology and evolution will need to address how space, migration
561 and/or fluctuating conditions affect the patterns of diversity. In addition, cooperation
562 between genotypes (such as cross-feeding or use of costly public goods) and many more

563 resources have the potential to shape diversity levels and should also be investigated in
564 future studies.

565

566

References

Abrams, P. A. (1988) 'How should resources be counted?', *Theoretical Population Biology*. doi: 10.1016/0040-5809(88)90014-7.

Amado, A. and Campos, P. R. A. (2019) 'Ecological specialization under multidimensional trade-offs', *Evolutionary Ecology*. Springer International Publishing, 33(6), pp. 769–789. doi: 10.1007/s10682-019-10013-4.

Mac Arthur, R. (1969) 'Species Packing, and What Competition Minimizes', *Proceedings of the National Academy of Sciences*, 64(4), pp. 1369–1371. doi: 10.1073/pnas.64.4.1369.

Bailey, S. F. and Kassen, R. (2012) 'Spatial structure of ecological opportunity drives adaptation in a bacterium', *American Naturalist*. doi: 10.1086/666609.

Barroso-Batista, J. *et al.* (2014) 'The First Steps of Adaptation of Escherichia coli to the Gut Are Dominated by Soft Sweeps', *PLoS Genetics*. doi: 10.1371/journal.pgen.1004182.

Barroso-Batista, J. *et al.* (2020) 'Specific Eco-evolutionary Contexts in the Mouse Gut Reveal Escherichia coli Metabolic Versatility', *Current Biology*. doi: 10.1016/j.cub.2020.01.050.

Bedhomme, S., Lafforgue, G. and Elena, S. F. (2012) 'Multihost experimental evolution of a plant RNA virus reveals local adaptation and host-specific mutations', *Molecular Biology and Evolution*. doi: 10.1093/molbev/msr314.

Bell, G. and Reboud, X. (1997) 'Experimental evolution in Chlamydomonas II. Genetic variation in strongly contrasted environments', *Heredity*. doi: 10.1038/hdy.1997.78.

Billiard, S. and Smadi, C. (2020) 'Stochastic dynamics of three competing clones: Conditions and times for invasion, coexistence, and fixation', *American Naturalist*, 195(3), pp. 463–484. doi: 10.1086/707017.

Bull, J. J., Badgett, M. R. and Wichman, H. A. (2000) 'Big-benefit mutations in a bacteriophage inhibited with heat', *Molecular Biology and Evolution*. doi: 10.1093/oxfordjournals.molbev.a026375.

Cheng, Y. (1995) 'Mean Shift, Mode Seeking, and Clustering', *IEEE Transactions on Pattern Analysis and Machine Intelligence*. doi: 10.1109/34.400568.

Chou, H. H. *et al.* (2011) 'Diminishing returns epistasis among beneficial mutations decelerates adaptation', *Science*, 332(6034), pp. 1190–1192. doi: 10.1126/science.1203799.

Coffey, L. L. *et al.* (2008) 'Arbovirus evolution in vivo is constrained by host alternation', *Proceedings of the National Academy of Sciences of the United States of America*. doi: 10.1073/pnas.0712130105.

Cohan, F. M. (2002) 'What are bacterial species?', *Annual Review of Microbiology*. doi: 10.1146/annurev.micro.56.012302.160634.

Desai, M. M., Fisher, D. S. and Murray, A. W. (2007) 'The Speed of Evolution and Maintenance of Variation in Asexual Populations', *Current Biology*. doi: 10.1016/j.cub.2007.01.072.

Dieckmann, U. and Doebeli, M. (1999) 'On the origin of speciesby sympatric speciation', *Science*, 400(July), pp. 0–3. doi: 10.1038/22521.

Doebeli, M. (2011) *Adaptive diversification (MPB-48), Adaptive Diversification (MPB-48)*. doi: 10.23943/princeton/9780691128931.001.0001.

Drake, J. W. (1991) 'A constant rate of spontaneous mutation in DNA-based microbes', *Proceedings of the National Academy of Sciences of the United States of America*. doi: 10.1073/pnas.88.16.7160.

Duffy, S., Turner, P. E. and Burch, C. L. (2006) 'Pleiotropic costs of niche expansion in the RNA bacteriophage Φ6', *Genetics*. doi: 10.1534/genetics.105.051136.

Dykhuizen, D. E. and Dean, A. M. (2004) 'Evolution of specialists in an experimental microcosm', *Genetics*. doi: 10.1534/genetics.103.025205.

Edwards, K. F. *et al.* (2018) 'Evolutionarily stable communities: a framework for understanding the role of trait evolution in the maintenance of diversity', *Ecology Letters*, 21(12), pp. 1853–1868. doi: 10.1111/ele.13142.

Etheridge, A. M., Pfaffelhuber, P. and Wakolbinger, A. (2012) 'How often does the ratchet click? Facts, heuristics, asymptotics', *Trends in Stochastic Analysis*, 70, pp. 365–390. doi: 10.1017/cbo9781139107020.016.

Farahpour, F. *et al.* (2018) 'Trade-off shapes diversity in ecoevolutionary dynamics', *eLife*, 7. doi: 10.7554/eLife.36273.

Felsenstein, J. (1974) 'The evolution advantage of recombination', *Genetics*. doi: 10.1093/genetics/78.2.737.

Friesen, M. L. *et al.* (2004) 'Experimental evidence for sympatric ecological diversification due to frequency-dependent competition in Escherichia coli', *Evolution*, 58(2), pp. 245–260. doi: 10.1111/ele.12430.

Garud, N. R. *et al.* (2019) 'Evolutionary dynamics of bacteria in the gut microbiome within and across hosts', *PLoS biology*, 17(1), p. e3000102. doi: 10.1371/journal.pbio.3000102.

Geritz, S. A. H. *et al.* (1998) 'Evolutionary singular strategies and the adaptive growth and branching of the evolutionary tree', *Evolutionary Ecology*, 12, pp. 35–57.

Goldford, J. E. *et al.* (2018) 'Emergent simplicity in microbial community assembly', *Science*. doi: 10.1126/science.aat1168.

Good, B. H. *et al.* (2012) 'Distribution of fixed beneficial mutations and the rate of adaptation in asexual populations', *Proceedings of the National Academy of Sciences of the United States of America*, 109(13), pp. 4950–4955. doi: 10.1073/pnas.1119910109.

Good, B. H. *et al.* (2017) 'The dynamics of molecular evolution over 60,000 generations', *Nature*. doi: 10.1038/nature24287.

Good, B. H., Martis, S. and Hallatschek, O. (2018) 'Adaptation limits ecological diversification and promotes ecological tinkering during the competition for substitutable resources', *Proceedings of the National Academy of Sciences of the United States of America*, 115(44), pp. E10407–E10416. doi: 10.1073/pnas.1807530115.

Gordo, I. (2019) 'Evolutionary change in the human gut microbiome: From a static to a dynamic view', *PLoS Biology*, 17(2), pp. 1–5. doi: 10.1371/journal.pbio.3000126.

Gordo, I. and Charlesworth, B. (2000) 'The degeneration of asexual haploid populations and the speed of Muller's ratchet', *Genetics*. doi: 10.1093/genetics/154.3.1379.

Goyal, S. *et al.* (2012) 'Dynamic mutation-selection balance as an evolutionary attractor', *Genetics*. doi: 10.1534/genetics.112.141291.

Greene, I. P. *et al.* (2005) 'Effect of Alternating Passage on Adaptation of Sindbis Virus to Vertebrate and Invertebrate Cells', *Journal of Virology*. doi: 10.1128/jvi.79.22.14253-14260.2005.

Gresham, D. *et al.* (2008) 'The repertoire and dynamics of evolutionary adaptations to controlled nutrient-limited environments in yeast', *PLoS Genetics*. doi: 10.1371/journal.pgen.1000303.

Haigh, J. (1978) 'The accumulation of deleterious genes in a population-Muller's Ratchet', *Theoretical Population Biology*, 14(2), pp. 251–267. doi: 10.1016/0040-5809(78)90027-8.

Haldane, J. B. S. and Fisher, R. A. (1931) 'The Genetical Theory of Natural Selection', *The Mathematical Gazette*. doi: 10.2307/3606227.

Hardin, G. (1960) 'The Competitive Exclusion Principle', *Science*, 131(November).

Herron, M. D. and Doebeli, M. (2013) 'Parallel Evolutionary Dynamics of Adaptive Diversification in

Escherichia coli', *PLoS Biology*. doi: 10.1371/journal.pbio.1001490.

Huston, M. A. (1994) 'Biological diversity: the coexistence of species on changing landscapes', *Biological diversity: the coexistence of species on changing landscapes*. doi: 10.2307/2404662.

Hutchinson, G. E. (1961) 'THE PARADOX OF THE PLANKTON * New Haven , Connecticut Osborn Zoological Laboratory , The problem that I wish to discuss in the present contribution is raised by the very paradoxical situation of the plankton , particularly the phyto- plankton , of relativ', XCV(882), pp. 137–145.

Ispolatov, I., Madhok, V. and Doebeli, M. (2016) 'Individual-based models for adaptive diversification in high-dimensional phenotype spaces', *Journal of Theoretical Biology*. Elsevier, 390, pp. 97–105. doi: 10.1016/j.jtbi.2015.10.009.

Johnson, Norman L *et al.* (1994) 'Continuous Univariate Distributions', *Wiley*, 1, p. Section 10.1.

Kassen, R. and Bell, G. (1998) 'Experimental evolution in Chlamydomonas. IV. Selection in environments that vary through time at different scales', *Heredity*. doi: 10.1046/j.1365-2540.1998.00329.x.

Kinnersley, M. A., Holben, W. E. and Rosenzweig, F. (2009) 'E unibus plurum: Genomic analysis of an experimentally evolved polymorphism in Escherichia coli', *PLoS Genetics*. doi: 10.1371/journal.pgen.1000713.

Kremer, C. T. and Klausmeier, C. A. (2017) 'Species packing in eco-evolutionary models of seasonally fluctuating environments', *Ecology Letters*. doi: 10.1111/ele.12813.

Kryazhimskiy, S. *et al.* (2014) 'Global epistasis makes adaptation predictable despite sequence-level stochasticity', *Science*, 344(6191), pp. 1519–1522. doi: 10.1126/science.1250939.

Lawrence, D. *et al.* (2012) 'Species interactions alter evolutionary responses to a novel environment', *PLoS Biology*. doi: 10.1371/journal.pbio.1001330.

Leónidas Cardoso, L. *et al.* (2020) 'Dysbiosis individualizes the fitness effect of antibiotic resistance in the mammalian gut', *Nature Ecology and Evolution*. Springer US, 4(9), pp. 1268–1278. doi: 10.1038/s41559-020-1235-1.

Li, Y., Petrov, D. A. and Sherlock, G. (2019) 'Single nucleotide mapping of trait space reveals Pareto fronts that constrain adaptation', *Nature Ecology and Evolution*. Springer US, 3(11), pp. 1539–1551. doi: 10.1038/s41559-019-0993-0.

Lisic, J. (2018) 'meanShiftR: A Computationally Efficient Mean Shift Implementation. R package version 0.53', pp. 1–5. Available at: https://cran.r-project.org/package=meanShiftR.

Litchman, E. and Klausmeier, C. A. (2001) 'Competition of phytoplankton under fluctuating light', *American Naturalist*. doi: 10.1086/318628.

MacQueen, J. (1967) 'Some methods for classification and analysis of multivariate observations', in *Proceedings of the fifth Berkeley Symposium on Mathematical Statistics and Probability*.

Maharjan, R. *et al.* (2006) 'Clonal adaptive radiation in a constant environment', *Science*. doi: 10.1126/science.1129865.

Nicholson, J. K. *et al.* (2012) 'Host-gut microbiota metabolic interactions', *Science*. doi: 10.1126/science.1223813.

de Oliveira, V. M., Amado, A. and Campos, P. R. A. (2018) 'The interplay of tradeoffs within the framework of a resource-based modelling', *Ecological Modelling*. Elsevier, 384(June), pp. 249–260. doi: 10.1016/j.ecolmodel.2018.06.026.

Pacciani-Mori, L. *et al.* (2020) 'Dynamic metabolic adaptation can promote species coexistence in competitive microbial communities', *PLoS Computational Biology*, 16(5), pp. 1–18. doi: 10.1371/journal.pcbi.1007896.

Park, S. C. and Krug, J. (2007) 'Clonal interference in large populations', *Proceedings of the National Academy of Sciences of the United States of America*, 104(46), pp. 18135–18140. doi: 10.1073/pnas.0705778104.

Perfeito, L. *et al.* (2007) 'Adaptive mutations in bacteria: High rate and small effects', *Science*, 317(5839), pp. 813–815. doi: 10.1126/science.1142284.

Philip J. Gerrish & Richard E. Lenski (1998) 'The fate of competing beneficial mutations in an asexual population', *Genetica*, 102/103, pp. 127–144,.

Posfai, A., Taillefumier, T. and Wingreen, N. S. (2017) 'Metabolic Trade-Offs Promote Diversity in a Model Ecosystem', *Physical Review Letters*, 118(2), pp. 1–5. doi: 10.1103/PhysRevLett.118.028103.

Reboud, X. and Bell, G. (1997) 'Experimental evolution in Chlamydomonas III. Evolution of specialist and generalist types in environments that vary in space and time', *Heredity*. doi: 10.1038/hdy.1997.79.

Rosindell, J., Harmon, L. J. and Etienne, R. S. (2015) 'Unifying ecology and macroevolution with individual-based theory', *Ecology Letters*, 18(5), pp. 472–482. doi: 10.1111/ele.12430.

Satterwhite, R. S. and Cooper, T. F. (2015) 'Constraints on adaptation of Escherichia coli to mixed-resource environments increase over time', *Evolution*, 69(8), pp. 2067–2078. doi: 10.1111/evo.12710.

Schoener, T. W. (2011) 'The Newest Synthesis: Understanding Ecological Dynamics', *Science*, 331(January), pp. 426–429. doi: 10.1126/science.1193954.

Schoustra, S. *et al.* (2016) 'Diminishing-returns epistasis among random beneficial mutations in a multicellular fungus', *Proceedings of the Royal Society B: Biological Sciences*, 283(1837). doi: 10.1098/rspb.2016.1376.

Shoresh, N., Hegreness, M. and Kishony, R. (2008) 'Evolution exacerbates the paradox of the plankton', *Proceedings of the National Academy of Sciences of the United States of America*, 105(34), pp. 12365–12369. doi: 10.1073/pnas.0803032105.

de Sousa, J. A. M. *et al.* (2016) 'Competition and fixation of cohorts of adaptive mutations under Fisher geometrical model', *PeerJ*, 2016(2), pp. 1–17. doi: 10.7717/PEERJ.2256.

Sunagawa, S. *et al.* (2015) 'Structure and function of the global ocean microbiome', *Science*. doi: 10.1126/science.1261359.

T. E. Sandberg, C. J. Lloyd, B..O. Palsson, A. M. F. (2017) 'Laboratory Evolution to Alternating Substrate Environments Yields Distinct Phenotypic and Genetic Adaptive Strategies', 83(13), pp. 1–15.

Tajima, F. (1989) 'Statistical method for testing the neutral mutation hypothesis by DNA polymorphism', *Genetics*.

Tilman, D. (1982) 'Resource competition and community structure.', *Monographs in population biology*. doi: 10.2307/4549.

Trindade, S. *et al.* (2009) 'Positive epistasis drives the acquisition of multidrug resistance', *PLoS Genetics*. doi: 10.1371/journal.pgen.1000578.

Turner, P. E. and Elena, S. F. (2000) 'Cost of host radiation in an RNA virus', *Genetics*.

Ward, H., Perron, G. G. and MacLean, R. C. (2009) 'The cost of multiple drug resistance in Pseudomonas aeruginosa', *Journal of Evolutionary Biology*. doi: 10.1111/j.1420-9101.2009.01712.x.

Whittaker, R. H. (1965) 'Dominance and diversity in land plant communities', *Science*. doi: 10.1126/science.147.3655.250.

Wright, S. (1938) 'The Distribution of Gene Frequencies Under Irreversible Mutation', *Proceedings of the National Academy of Sciences*. doi: 10.1073/pnas.24.7.253.

Wünsche, A. *et al.* (2017) 'Diminishing-returns epistasis decreases adaptability along an evolutionary trajectory', *Nature Ecology and Evolution*, 1(4), pp. 1–6. doi: 10.1038/s41559-016-0061.

Zhao, S. *et al.* (2019) 'Adaptive Evolution within Gut Microbiomes of Healthy People', *Cell Host and Microbe*. Elsevier Inc., 25(5), pp. 656-667.e8. doi: 10.1016/j.chom.2019.03.007.

Figures

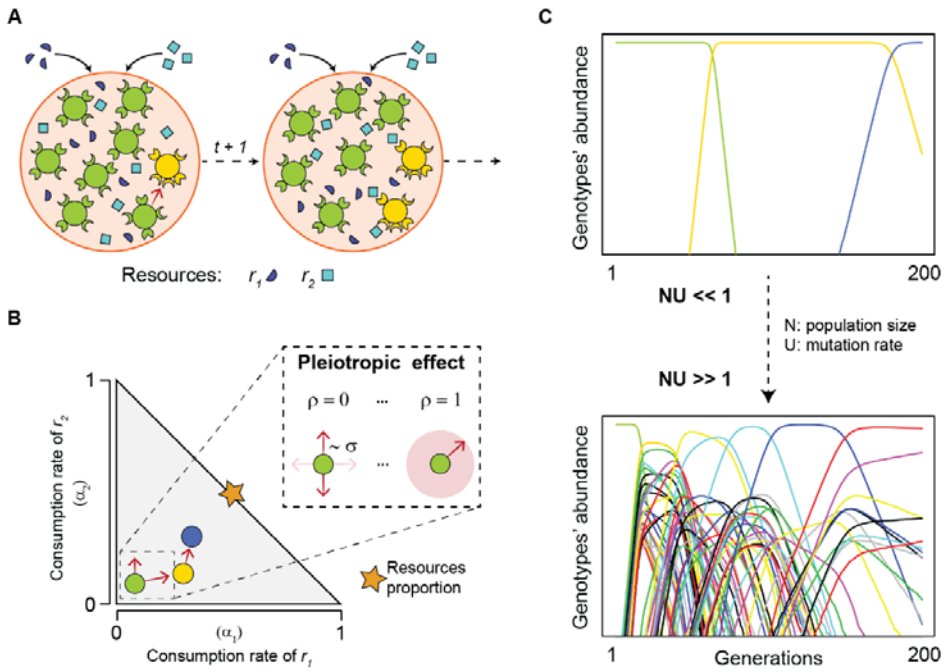

Figure 1. **Ecological dynamics and individual-based evolutionary processes**. **A)** Illustration of the eco-evolutionary dynamics. Bacterial genotypes, represented by circles of different colors, grow according to the constant input of resources (squares and semicircles) and their phenotypic traits, represented by the enzyme-like structures on the circles. Mutation events (red arrow) can generate new types whose fate will depend on drift and selection. **B)** Constrained phenotypic space and mutation process. An initially maladapted monomorphic population (green circle) can acquire de-novo mutations according to the given assumptions (as explained in the inset) and move inside the phenotypic space with an upper bound on the total energy. **C)** Examples of different mutation regimes: from low/absent (NU << 1) to extensive (NU >>1) clonal interference. Each color represents a different genotype.

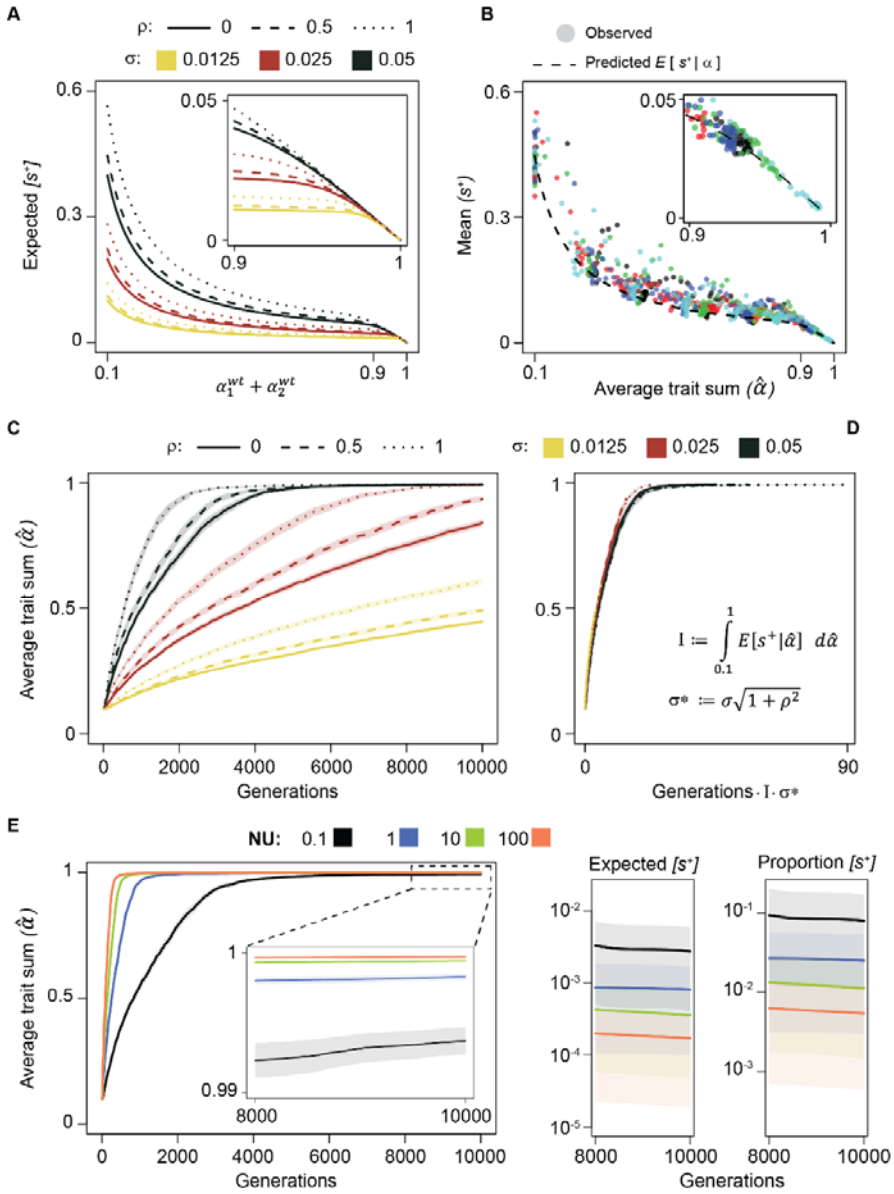

Figure 2. Diminishing return epistasis and the adaptation rate. A) Analytical predictions of the diminishing return epistasis in monomorphic populations. The inset shows the effect of the energy constraint. **B)** Dots represent the mean of the observed positive selection during the first 300 generations of adaptation. The dotted line represents the prediction using the average population trait sum $\left(\hat{\alpha}(t) := \frac{\sum_i^{M(t)} n_i(t)(\alpha_1^{(i)}+\alpha_2^{(i)})}{N}\right)$. Each color represents an independent simulated population, which adapted with $\sigma = 0.05$, $\rho = 0.5$, $N = 10^7$ and U= 10^{-5}. **C)** The population average trait sum $\hat{\alpha}(t)$ is shown as proxy of adaptation under different σ and ρ conditions. Other parameters: $R = 2$, $N = 10^7$, $U = 10^{-8}$. Lines are the averages over 100 simulations and the shaded areas represent the confidence interval. **D)** Same dynamics as in C, but on a different scale, as defined in the figure. **E)** Phenotypic adaptation across different mutational inputs (left) and expected strength and proportion of beneficial mutations at the end of the adaptation process. Other parameters for panel E: $N = 10^7$, $\sigma = 0.05$, $\rho = 0.5$.

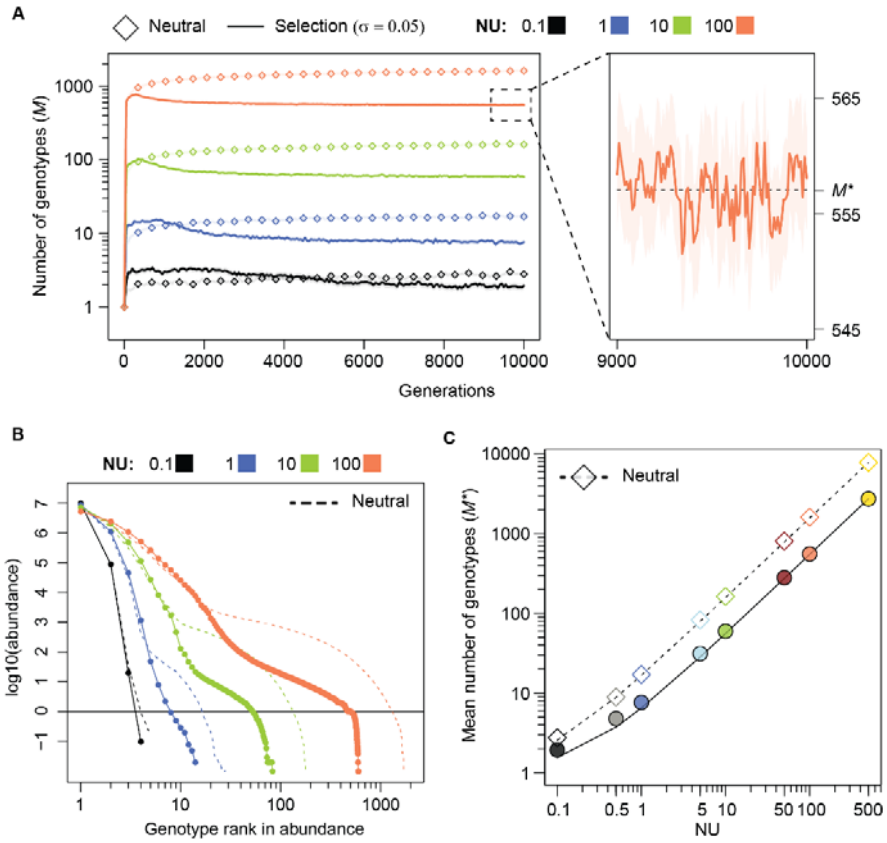

Figure 3. Genotypes' dynamics and balance under competition for two resources. A) Number of genotypes present in the environment over time, under neutrality (diamonds) or under selection (lines). Lines represent the average across 100 populations and the shaded area their confidence interval. On the right, zoom over the last 1000 generation. Other parameters: $\sigma = 0.05, \rho = 0$ and $N = 10^7$. **B)** Log-log scaled rank abundance distribution of genotypes at generation 10000. Dots and dashed lines represent the mean across 100 populations under selection or neutrality, respectively. Parameters as in A. **C)** Long-lasting number of genotypes, computed as the average over the last 1000 generations (e.g. dotted line in the right panel of A). The lines represent the linear regressions: $M^* = aNU + 1$ where NU: $\{0.1, 0.5, 1, 5, 10, 50, 100, 500\}$ and $a = \{15.70 \pm 0.07, 5.48 \pm 0.02\}$ for the neutral or selection cases, respectively. Both axes are represented in *log* scale with ticks every $\{1, \ldots, 9\} \cdot 10^x$. Other parameters as in A.

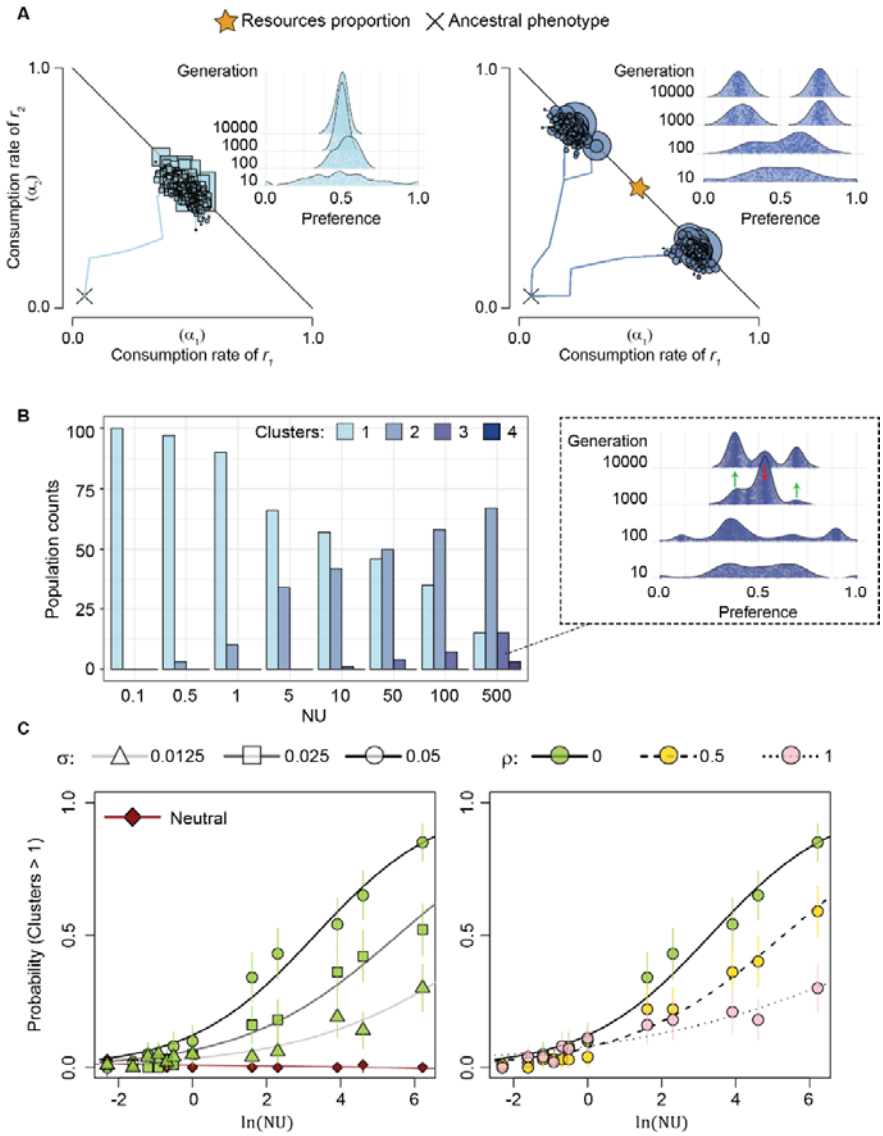

Figure 4. Ecological diversification under competition for two resources. A) Two example populations evolving under the same conditions ($N = 10^7, U = 10^{-5}, \rho = 0.5, \sigma = 0.05, \mathrm{R} = 2$). The phenotypes and the preference distributions show one population that has evolved into a single optimal cluster (squares) and another population that gave rise to a stable diverse community composed by two clusters (circles). Lines connecting the shapes represent mutations. **B)** Counts of populations that evolved into 1,2 or more phenotypic clusters. Here, $N = 10^7, \sigma = 0.05, \mathrm{R} = 2, \rho = 0$. **C)** Populations diversify with a probability that increases with $\ln(NU)$ and σ but decreases with ρ. The lines represent the fit of the data to the logistic function: $P = \frac{1}{1+e^{a(\ln(NU)-b)}}$, NU: $\{0.1, 0.2, 0.3, 0.4, 0.5, 0.6, 1, 5, 10, 50, 100, 500\}$. The inferred parameters a and b are reported in Tables S1-2 and the full set of data is shown in Fig. S5. In the left plot: $\rho = 0$, while in the right one: $\sigma = 0.05$. The probabilities were computed as proportions out of

100 independent populations and their 95% confidence interval by normal approximation: $P \pm z\sqrt{\frac{P(1-P)}{100}}$, $z = 1.96$.

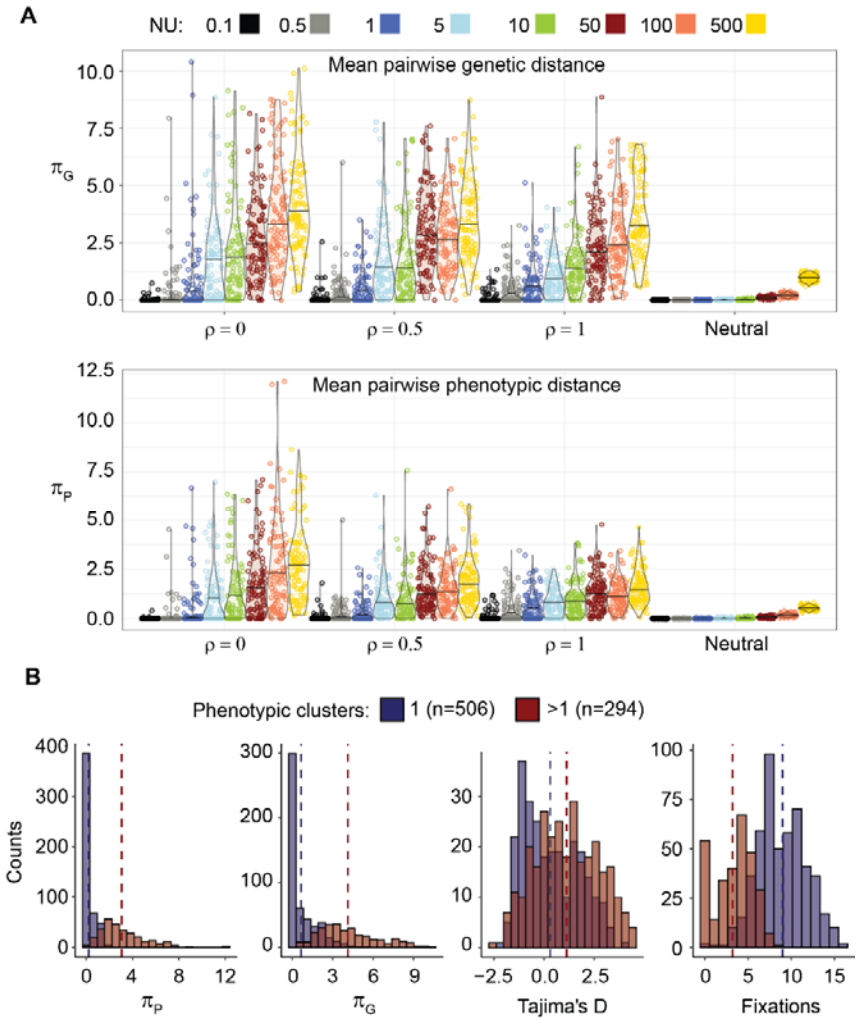

Figure 5. Phenotypic and genetic characterization of the evolved populations. A) Average pairwise genotypic (π_G) and phenotypic (π_P) diversity were measured within each population, as defined in the *Methods*. 100 independent populations were simulated for each of the conditions specified on the x axis and by the colors. Other parameters: σ = 0.05, 2 resources and $N = 10^7$. **B)** π_P, π_G, Tajima's D and fixations distributions of the populations that evolved into a single cluster (blue, n=506) or into multiple ones (red, n=294). Populations with different NU and ρ=0 were pulled together for a total of 800 populations. The dotted lines represent the means of the corresponding distribution.

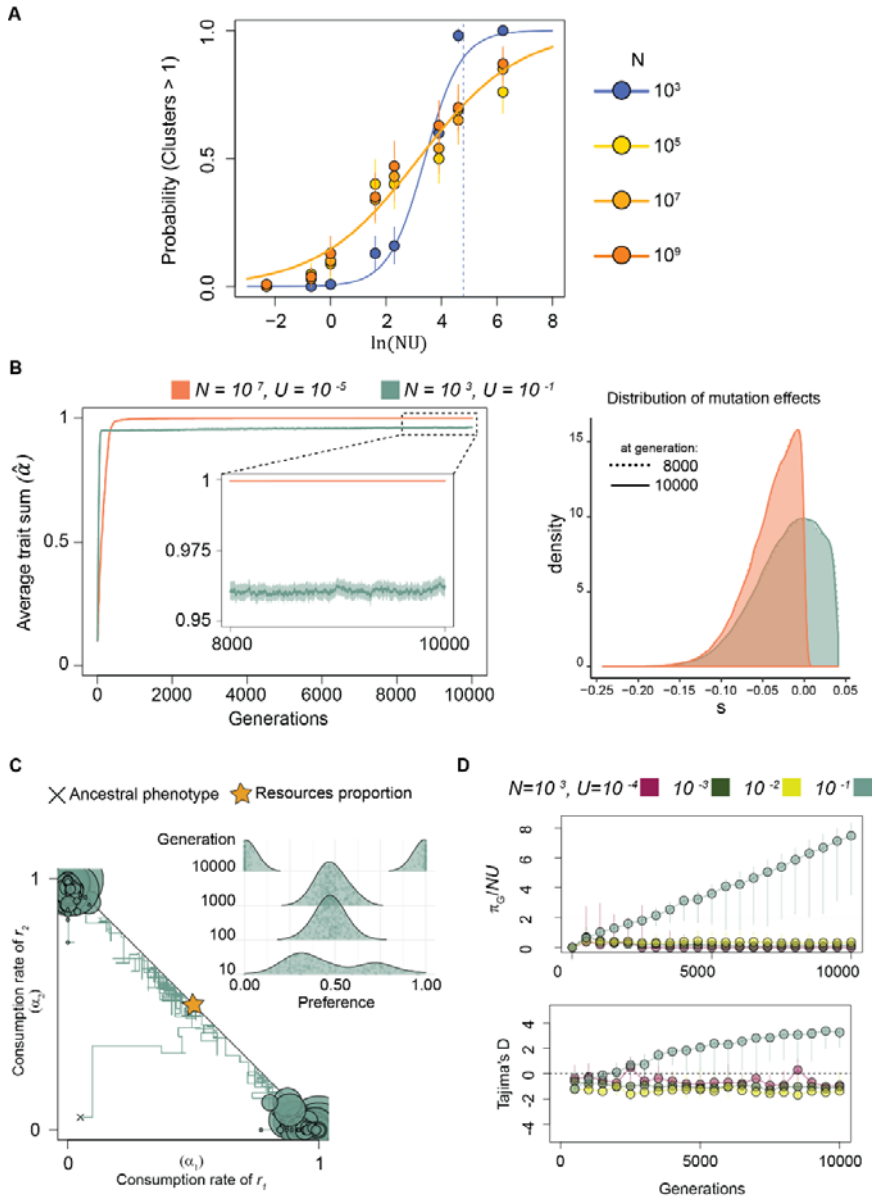

Figure 6. **Speciation process in small populations with large mutational input. A)** Probability of diversification across different population sizes. Continuous lines represent the fit of the data to the logistic function: $P = \frac{1}{1+e^{a(\ln(NU)-b)}}$, NU: {0.1, ,0.5, 1, 5,10, 50,100, 500}, for $N = 10^3$ (blue) or $N = 10^5, 10^7, 10^9$ together (orange). The inferred parameters a and b are reported in Tables S3. The dotted line represents the threshold ($\ln(NU) = 4.78$) when $\frac{NU}{Ns \cdot \ln(NU)} > 0.5$, $N = 10^3$ and $s = \sigma$. The probabilities were computed as for Fig. 4. **B)** Average trait sum over time and distribution of mutation effects at generations 8000 or 10000. **C)** Example population adapted with $N = 10^3, U = 10^{-1}, \rho = 0, \sigma = 0.05, R = 2$ for 10000 generations. The inset shows the preference distribution at generations 10, 100, 1000 and 10000. **D)** π_G/NU and Tajima's D over time. Circles represent the median, while vertical bars range from the 25th to the 75th quartiles. The dotted lines represent the expected value at neutral equilibrium. In particular $\pi_G = 2NU$ and Tajima's D=0. Other parameters: $\sigma = 0.05, \rho = 0$.